ACS APPLIED MATERIALS & INTERFACES

Research Article

Cite This: ACS Appl. Mater. Interfaces 2018, 10, 17463−17470

www.acsami.org

Investigation on the Linker Length of Synthetic Zwitterionic Polypeptides for Improved Nonfouling Surfaces

Chong Zhang, Jianhua Lu, Yingqin Hou, Wei Xiong, Kai Sheng, and Hua Lu*

Beijing National Laboratory for Molecular Sciences, Center for Soft Matter Science and Engineering, Key Laboratory of Polymer Chemistry and Physics of Ministry of Education, College of Chemistry and Molecular Engineering, Peking University, Beijing 100871, People's Republic of China

Supporting Information

ABSTRACT: Zwitterionic polymers are outstanding nonfouling materials widely used for surface modification. However, works that systematically evaluate the structure−activity relationship of the side chain linker effect with related antifouling abilities are sparse. Here, we generate a series of well-defined zwitterionic polypeptides bearing oligoethylene glycol (EG) linkers in the side chain (P(CB-EG$_x$Glu), x = 1−3) and anchor them on gold surfaces via the grafting-to approach to compare their antifouling performances. The surface properties are characterized by X-ray photoelectron spectroscopy (XPS), circular dichroism spectroscopy (CD), variable angle spectroscopic ellipsometry (VASE), static water contact angle (SCA), and atomic force microscopy (AFM). By use of quartz crystal microbalance with dissipation (QCM-D), confocal microscopy, and scanning electron microscope, our results convincingly demonstrate the excellent antifouling performance of all zwitterionic polypeptides. Importantly, the surface coated with P(CB-EG$_3$Glu), the one with the longest EG linker, exhibits the best resistance to single protein (below the detection limit of QCM) and blood serum (~96−98% reduction) adsorption, which largely outperforms those of the PEG positive control and the two P(CB-EG$_x$Glu) analogues with shorter EG$_x$ linkers. The same P(CB-EG$_3$Glu) surface also gives the highest degree of prevention of cell/platelet/bacterial attachment (~99% reduction) among all samples tested. Together, our study highlights the linker effect to the nonfouling performance of zwitterionic polypeptides, and the results strongly support P(CB-EG$_3$Glu) as a robust nonfouling material for numerous applications.

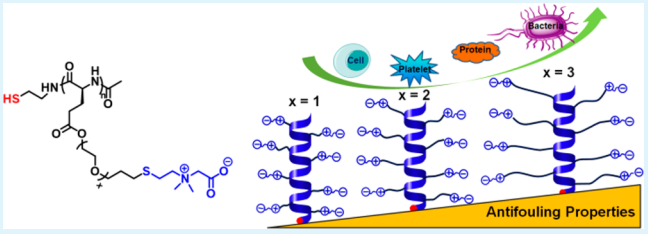

KEYWORDS: *polypeptides, zwitterion, protein-resistant, nonfouling surfaces, linker chemistry*

INTRODUCTION

Biofouling of medical devices, implants, and warships can significantly compromise their performance and cause numerous problems such as tissue fibrosis, bacterial infection, and inefficient fuel consumption.[1−4] Surface modification with antifouling polymers is a common strategy to minimize problems arising from such biofouling.[5−10] Zwitterionic polymers, which have both cation and anion moieties on the same monomer unit with an overall neutral charge, have been extensively explored as excellent nonfouling materials.[11−14] Moreover, such polymers have also been widely used in nanoparticle surface coating and protein conjugation to improve their circulation half-lives and stealth properties.[15−17] Presumably, the zwitterionic polymers can generate a more tightly bound water layer through the electrostatically induced hydration and thus impart outstanding antifouling properties under complex biological environments.[18,19] Nevertheless, most zwitterionic polymers investigated are nondegradable vinyl polymers. In addition, the side chain linkers between the zwitterion and the polymeric backbone are generally hydrophobic and very short (~5 σ bonds), and there have been very few reports optimizing their linker chemistry for enhanced nonfouling performances.[20−22]

Synthetic polypeptides are degradable and biocompatible protein-mimicking polymers with versatile side chain structures, tunable properties, and numerous functions.[23−26] Owing to recent advances in synthetic technologies, the ring-opening polymerization (ROP) of α-amino acid N-carboxyanhydrides (NCAs) has become a facile and powerful tool to generate libraries of polypeptides for numerous applications.[27−32] To this end, we reason that zwitterionic polypeptides are promising candidates to interrogate the effect of linker chemistry for antifouling purposes. Herein, we report the synthesis and comparative studies of a series of novel zwitterionic polypeptides bearing carboxy betaine (CB) and varied lengths of oligoethylene glycol (EG$_x$) linkers, denoted as P(CB-EG$_x$Glu) (x = 1, 2, and 3). By integrating both the hydrogen bonding (EG$_x$) and ionic solvation (zwitterion), we expect that the polymer with the longest EG linker (x = 3) can offer significantly improved nonfouling properties as compared to its analogues with shorter linkers (x = 1 and 2).[33]

Received: February 16, 2018
Accepted: May 8, 2018
Published: May 8, 2018

Downloaded via PEKING UNIV on October 14, 2018 at 03:18:40 (UTC).
See https://pubs.acs.org/sharingguidelines for options on how to legitimately share published articles.

© 2018 American Chemical Society

DOI: 10.1021/acsami.8b02854
ACS Appl. Mater. Interfaces 2018, 10, 17463−17470

EXPERIMENTAL SECTION

Materials. All reagents were obtained from commercial sources unless otherwise specified. Ultrapure Milli-Q water (Millipore, 18.2 MΩ cm) was used for all of the experiments. Hexamethyldisilazane (HMDS) and anhydrous *N*,*N*-dimethylformamide (DMF) were obtained from Sigma-Aldrich (St. Louis, MO) and used as received. The synthesis of *N*,*N*-dimethyl-cysteamine-carboxybetaine (CB-SH),[34] 2-(tritylthio)ethanamine,[35] L-EG$_x$ene-GluNCA (x = 1, 2, and 3), and the dn/dc values of P(EG$_x$ene-Glu)[36] were reported in separated works. Bovine serum albumin (BSA), human plasma fibrinogen, phosphate buffered saline (PBS, pH 7.4 at 25 °C), and human serum were purchased from Solarbio Science and Technology (Beijing, China).

Instrumentation. Nuclear magnetic resonance (NMR) experiments were recorded on an AVANCE 400 spectrometer (Bruker Biospin, Switzerland). Fourier transform infrared spectroscopy (FT-IR) experiments were conducted on a FT-IR spectrometer (Bruker Tensor 27, Bremen, Germany) in transmission mode in the 400−4000 cm^{-1} range at a resolution of 2 cm^{-1} and 64 scans. Circular dichroism (CD) spectra were collected on a CD spectrometer (Bio-Logic MOS 450, Grenoble, France) using a 1.0 cm path length quartz cells at room temperature. The CD spectra of polymer coatings were recorded by placing four polymer-coated quartz wafers (to increase the signal intensity) into a 1.0 cm path length quartz cuvette and immersing into PBS buffer.[37] Gel permeation chromatography (GPC) analysis were carried out on a system equipped with an isocratic pump (Model 1100, Agilent Technology, Santa Clara, CA), a multiangle laser light scattering (Wyatt Technology, Santa Barbara, CA), and an Optilab rEX refractive index detector (Wyatt Technology, Santa Barbara, CA). DMF containing 0.1 M LiBr was used as the mobile phase and eluted at 50 °C with 1.0 mL/min flow rate. The XPS spectra were collected on an Axis Ultra X-ray photoelectron spectrometer (Kratos Analytical Ltd., Japan). All binding energies were calibrated using the C (1s) carbon peak (284.8 eV). The static water contact angles of the surfaces were measured using a Kruss DSA-100 goniometer with a water droplet volume of 2.0 μL and an equilibration time of 10 s at room temperature. The results were averaged from at least three measurements. Statistical significance was determined by two-way ANOVA analysis, and the differences were considered statistically significant at $p \leq 0.05$. The ellipsometry spectra were recorded using a M2000 V variable angle spectroscopic ellipsometry (VASE) from J.A. Woollam Co. (Lincoln, NE). All measurements were performed across the wavelength range 370−1000 nm at two angles of incidence 70° and 80°. The ellipsometric data were analyzed using the Cauchy model with the parameters A_n and B_n were set as 1.45 and 0.01, respectively.[38] The dried thickness of coating was obtained by measuring at least three independent samples and expressed as mean ± standard deviation (SD). The surface topographies and roughnesses were analyzed by a Bruker Dimension FastScan atomic force microscope (AFM, Germany). The surface morphology was studied using a field-emission scanning electron microscope (FE-SEM, ZEISS, Germany).

Polymer Synthesis. *Synthesis of P(EG$_x$ene-Glu)-S-Trt.* To a stirred solution of L-EG$_1$eneGlu-NCA (100 mg, 0.39 mmol, 50 equiv) in dry DMF (2 mL) in a glovebox was added 2-(tritylthio)ethanamine (15.6 μL × 0.5 M in DMF, 1.0 equiv) at room temperature. Acetic anhydride (14.8 μL, 0.16 mmol, 20 equiv) was added to terminate the reaction (2 h), after which the monomer was completely consumed. The crude product was obtained by adding the polymer solution dropwise to an excess of diethyl ether and followed by centrifugation. After washing with diethyl ether for totally three times, the obtained P(EG$_1$ene-Glu)-*S*-Trt was collected and dried in a vacuum oven in ∼75% isolated yield. P(EG$_2$ene-Glu)-*S*-Trt and P(EG$_3$ene-Glu)-*S*-Trt were synthesized by following the same procedure.

Synthesis of P(CB-EG$_x$Glu)-S-Trt. To a stirred solution of P(EG$_1$ene-Glu)-*S*-Trt (20.0 mg, 0.094 mmol "ene") and 2,2-dimethoxy-2-phenylacetophenone (DMPA, 2.3 mg, 0.009 mmol) in 2.0 mL of DMF was added CB-SH (83.3 mg, 0.47 mmol "thiol") in 0.8 mL of H_2O under a nitrogen atmosphere. The vials was capped and irradiated with1.0 W/cm^2 UV lamp for 6 h. After resupply of 3.0 mL of H_2O and 2.3 mg of DMPA, the reaction was irradiated for another 6 h to ensure complete modification. The product was purified by passing the diluted reaction mixture through a PD-10 column and then lyophilized (yield 70−85%). P(CB-EG$_2$Glu)-*S*-Trt and P(CB-EG$_3$Glu)-*S*-Trt were synthesized by the same procedure.

Synthesis of P(CB-EG$_x$Glu)-SH. In a 25 mL round-bottom flask was placed P(CB-EG$_1$Glu)-*S*-Trt (20 mg) in dichloromethane/trifluoroacetic acid (2.0/1.5 mL). The solution was cooled in an ice bath under nitrogen before triethylsilane (TES, 10 μL) was added. The reaction was allowed to stir at room temperature for 6 h. The polymer was collected by precipitation in a large amount of diethyl ether and dried in vacuum oven (yield ∼85%). P(CB-EG$_2$Glu)-SH and P(CB-EG$_3$Glu)-SH were synthesized by the same procedure.

Coating Preparation. Prior to surface modification, the gold chips were first cleaned in piranha solution (7/3, concentrated H_2SO_4/30% H_2O_2, v/v) at 60 °C for 15 min, followed by rinsing with distilled water, and dried with nitrogen stream. The gold chips were soaked into 1.0 mg/mL polymer solutions in PBS at room temperature for 12 h. Then, the polymer-grafted chips were exhaustively washed with water and dried with N_2. The P(CB-EG$_x$Glu)-coated quartz wafers were prepared according to the method reported previously.[39] Briefly, the cleaned quartz wafer was first functionalized with 3-(trimethoxysilyl)propyl acrylate (TPA) and then immersed in P(CB-EG$_x$Glu)-SH solutions (1.0 mg/mL in PBS) for 12 h to graft the polymers on the surfaces through Michael-type thiol−ene addition.

***In Situ* Monitoring of Polymer Adsorption.** Quartz crystal microbalance with dissipation (QCM-D, Q-Sense E4, Sweden) was used to monitor the polymer adsorption process in real time. Before the experiments, the QCM chip was first treated with piranha solution. The freshly cleaned chips were mounted into the flow chamber and exposed to PBS buffer until a stable baseline was obtained before the adsorbate solution was injected (1.0 mg/mL in PBS, 50 μL/min) at 25 °C. After 1 h of adsorption, the flow chamber was pumped with PBS buffer again. The 3rd, 5th, 7th, 9th, 11th, and 13th overtones were recorded, and only the 5th overtone was used to calculate the adsorbed mass. Because the $\Delta D/\Delta f$ ratio was relatively small ($\leq 4 \times 10^{-7}$ Hz^{-1}), the Sauerbrey equation was applied to calculate the hydrated adsorbed mass (Δm, ng/cm^2) of the surface coating ($\Delta m = -C \times \Delta f$, where C = 17.7 ng/(cm^2 × Hz) and Δf is the shift in frequency in the buffer baselines before and after polymer adsorption).[40−42]

Antifouling Test. *Protein Adsorption Assay.* QCM-D was used to examine the protein adsorption on the surface. The bare and modified QCM chips were inserted into the flow chambers and incubated with PBS buffer to obtain the baseline with a flow rate of 50 μL/min at 25 °C. The freshly prepared protein solutions (1.0 mg/mL BSA, 1.0 mg/mL fibrinogen, and 10% or 100% human serum) were pumped into the flow chamber. After 15 min of polymer adsorption, the chips surfaces were rinsed with PBS buffer for another 15 min. The QCM-D data were fitted using Qtools3 software (Version: 3.0.10.286) with Voigt viscoelastic model to calculate the amount of adsorbed protein. Three separate chips were tested to calculate the mean values and standard deviations for each coating (SD).

Cell Adhesion Experiments. The test gold substrates were placed into a 24-well tissue culture polystyrene (TCPS) plate after sterilized by 70% ethanol. Then, HeLa-eGFP cells were seeded onto the substrates with 10 000 cells per well in triplicate and substantially cultured at 37 °C in humidified atmosphere with 5% CO_2 for 24 h; the substrates were gently washed with PBS to remove any nonadherent cells. The attached cells on the gold substrates were observed using a confocal laser scanning microscope (Nikon A1R, Nikon Corp., Japan). At least three images from random locations were selected to calculate the fluorescence intensity for each sample, which was normalized to the unmodified surface.

Platelet Adhesion Experiments. The platelet-rich plasma (PRP) was obtained from freshly citrated rat blood by centrifuged for 10 min at 1000 rpm. After being equilibrated with PBS buffer for 2 h, PRP (400 μL) was added to the tested substrate and incubated at 37 °C for another 2 h. After gently rinsing with PBS buffer, the adherent platelets on the substrates were fixed with 2.5 wt % glutaraldehyde overnight,

DOI: 10.1021/acsami.8b02854
ACS Appl. Mater. Interfaces 2018, 10, 17463−17470

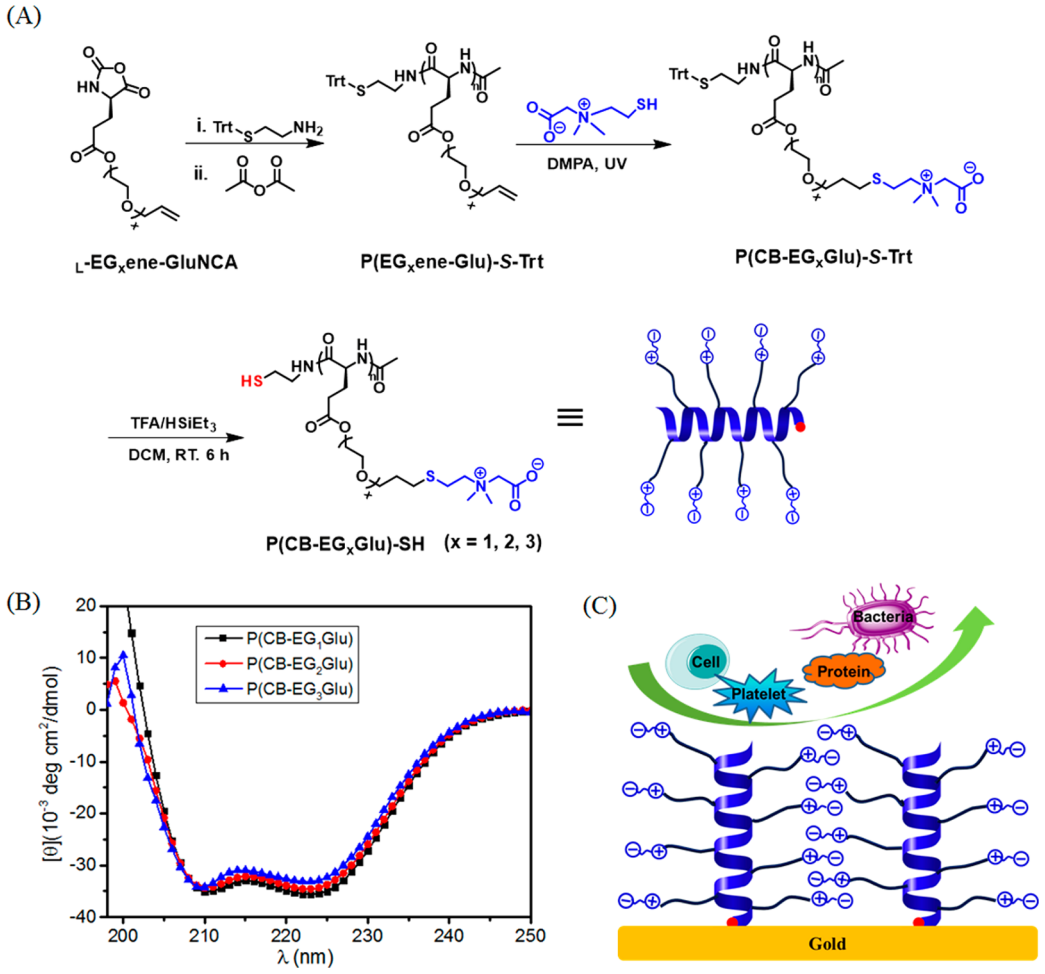

Figure 1. (A) Synthesis of the zwitterionic polypeptides P(CB-EG$_x$Glu). (B) CD spectra of the zwitterionic polypeptides P(CB-EG$_x$Glu) (PBS, pH = 7.4). (C) Cartoon illustration of self-assembled zwitterionic P(CB-EG$_x$Glu) coatings on gold surfaces.

followed by dehydrating with a series of ethanol aqueous solution (25%, 50%, 75%, 95%, and 100%, 20 min each). The adhered platelets on the surface were observed by SEM.

Bacterial Cell Adhesion Experiments. The *Escherichia coli* (*E. coli*) cells (10^6 cells/mL, 1.0 mL) were seeded onto the tested gold substrates that placed in a 24-well TCPS plate and incubated at 37 °C for 24 h. The surfaces were then gently washed with sterile PBS and the adhered bacteria were then fixed by immersing into 2.5 wt % glutaraldehyde overnight. The fixed bacteria were then dehydrated with a series of ethanol aqueous solution (25%, 50%, 75%, 95%, and 100%, 20 min each). After drying with a stream of nitrogen, the surface attached bacteria were observed by SEM.

RESULTS AND DISCUSSION

Synthesis and Characterization of the Zwitterionic Polypeptides. We selected EG$_x$ (x = 1, 2, and 3) as the linker in our zwitterionic polypeptides because PEG was a well-known polymer widely used for stealth purposes including nonfouling surfaces. By varying the number of the repeating unit of EG$_x$, the hydrophilicity, length, and steric hindrance of the side chain could be facilely adjusted. Briefly, the three zwitterionic polypeptides P(CB-EG$_x$Glu) were synthesized via the post-polymerization modification of three allyl-functionalized polypeptides P(EG$_x$ene-Glu), which were prepared from the ROP of corresponding L-EG$_x$ene-GluNCA monomers (x = 1, 2, and 3, Figure 1A). 2-(Tritylthio)ethanamine was selected as the initiator to introduce a thiol group for future gold surface anchoring. As shown in Table S1, the molecular weights (MWs) of P(EG$_x$eneGlu) measured by GPC (Figure S1) were in good agreement with the theoretical values, and all polymers were found to have narrow polydispersity indexes ($Đ$ < 1.10). Next, quantitative side chain functionalization was achieved using the highly efficient thiol−ene chemistry, as supported by the complete disappearance of the ally peaks (6.0−5.86 and 5.11−5.34 ppm) and the appearance of peaks belonging to the zwitterionic moieties in ^{1}H NMR spectroscopy (Figures S2−S4). Using a standard deprotection procedure, the thiol-terminated zwitterionic polypeptides P(CB-EG$_x$Glu) were obtained in high yield. Interestingly, all zwitterionic polypeptides adopted a typical α-helical conformation as verified by the CD spectroscopy (Figure 1B). The helical contents of all P(CB-EG$_x$Glu) were calculated to be above 90% (Table S1). Moreover, the helicity of the zwitterionic polypeptides remained almost unchanged under a wide range of proton and salt concentrations (Figure S5). This high helical stability was very similar to the ionic helical polypeptides developed by Cheng and co-workers.[43] Thus, the zwitterionic polypeptides P(CB-EG$_x$Glu) shared identical degree of polymerization (DP), primary and secondary backbone structures, which left the side chain chemistry the only variable structural parameter for a fair comparison (Figure 1C).

Characterization of P(CB-EG$_x$Glu)-Coated Surfaces. Next, we prepared the P(CB-EG$_x$Glu)-coated surfaces by

DOI: 10.1021/acsami.8b02854
ACS Appl. Mater. Interfaces 2018, 10, 17463−17470

Table 1. Quantitative Analysis of XPS Atomic Compositions of Zwitterionic Polypeptide-Modified Gold Surfaces

	XPS chemical composition (%)					molar ratios			
sample	Au 4f	C 1s	N 1s	O 1s	S 2p	N/Au	O/C	O/N	C−N$^+$/NH−C═O[a]
unmodified gold	66.31	27.42	1.19	5.08		0.018	0.19	4.27	
P(CB-EG$_1$Glu)	30.66	47.79	4.65	15.83	1.07	0.152	0.33	3.40	0.89
P(CB-EG$_2$Glu)	30.06	47.58	4.49	16.91	0.96	0.149	0.36	3.77	0.99
P(CB-EG$_3$Glu)	30.79	46.16	4.24	18.09	0.72	0.138	0.39	4.27	0.92

[a]Determined by the corresponding N 1s high-resolution spectra.

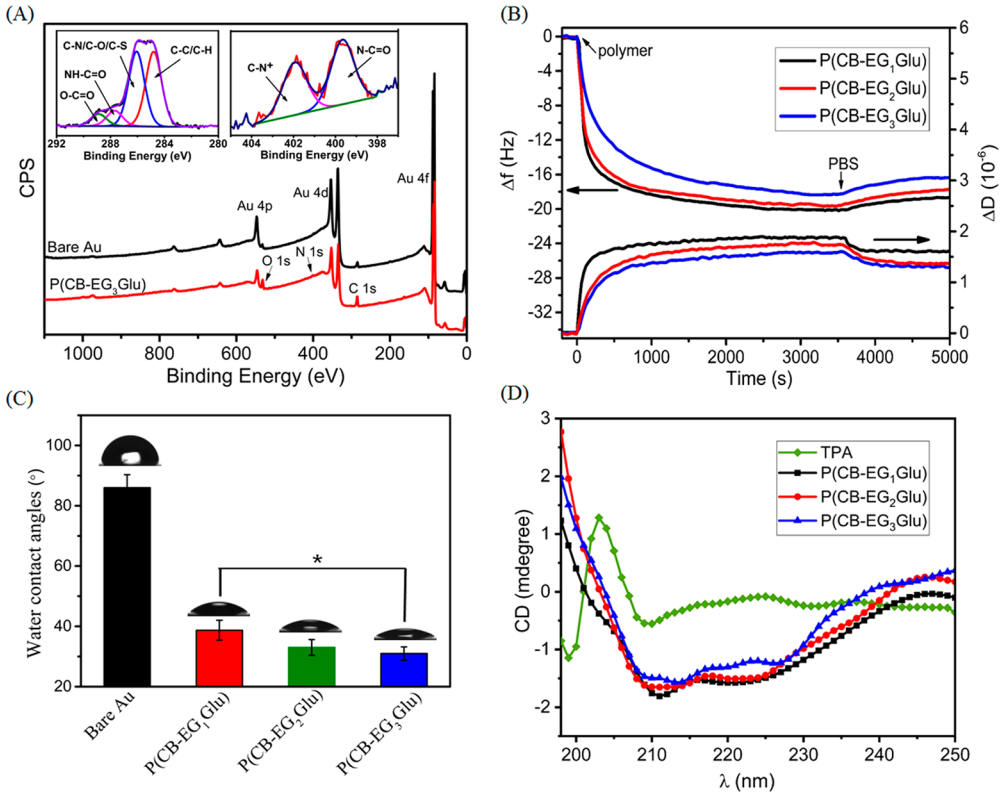

Figure 2. (A) XPS spectra of bare gold and P(CB-EG$_3$Glu)-coated surfaces (Inset: deconvolution of the C 1s and N 1s signals of the P(CB-EG$_3$Glu) coating). (B) In situ analysis of polymer adsorption on gold surface by QCM-D. (C) SCAs of all gold surfaces before and after modification with the zwitterionic polypeptides P(CB-EG$_x$Glu). The indicated p value (*p < 0.05) was calculated by two-way ANOVA analysis. (D) CD spectra of TPA- and P(CB-EG$_x$Glu)-coated quartz wafers.

directly incubating the gold chips with corresponding polymer solutions. XPS measurement of the surfaces in dry state indicated the successful formation of the polymer coatings (Table 1, Figure 2A, and Figure S6). After polymer modification, substantial increases of C 1s, N 1s, and O 1s signals, accompanied by a decrease in Au 4f concentration, were observed. Figure 2A shows the representative XPS narrow scans of the C 1s and N 1s signals. Deconvolution of the C 1s scan resulted in four component peaks attributable to C−C/C−H, C−N/C−O/C−S, the amide NH−C═O, and the ester O−C═O.[44] The N 1s scan was also resolved into two typical peaks attributed to the amide NH−C═O and the quaternary ammonium,[45] which was derived from the polypeptide backbone and the zwitterionic CB group, respectively. The atomic ratios of O/C and O/N and the XPS-derived molar ratios of C−N$^+$/NH−C═O were very close to the theoretical values for all coatings. Given the P(CB-EG$_x$Glu) polymers shared a similar DP, the grafting density could be roughly estimated by comparing the N/Au ratio of the P(CB-EG$_x$Glu)-coated surfaces. It was found that the N/Au ratio decreased slightly as the linker was extended from EG$_1$ to EG$_3$, suggesting P(CB-EG$_1$Glu) had a higher grafting density (number of polymer chain per area) than P(CB-EG$_3$Glu) at room temperature. To further confirm this, we measured the dry thickness of all surfaces by VASE. It was found that the thickness decreased from 24.6 to 16.5 Å when the EG$_x$ linker of P(CB-EG$_x$Glu) was elongated from 1 to 3 (Figure S7). This, in turn, implied that P(CB-EG$_1$Glu) had the highest dry mass among the three, ~149% of the mass of P(CB-EG$_3$Glu) coated on surfaces if we assume the polymers share the same bulk density. This was expectable because the latter polymer had a longer side chain and would occupy more space on surface than the former one.

Next, to investigate the hydrated mass of the polymer coatings we employed QCM to monitor the *in situ* adsorption of the adsorbents. As shown in Figure 2B, P(CB-EG$_1$Glu) exhibited a faster adsorption rate and a greater adsorption mass than its analogues with longer EG$_x$ linkers. Interestingly, the hydrated mass of P(CB-EG$_1$Glu) on surface was ~119% of that of P(CB-EG$_3$Glu), and this difference was appreciably smaller

DOI: 10.1021/acsami.8b02854
ACS Appl. Mater. Interfaces 2018, 10, 17463−17470

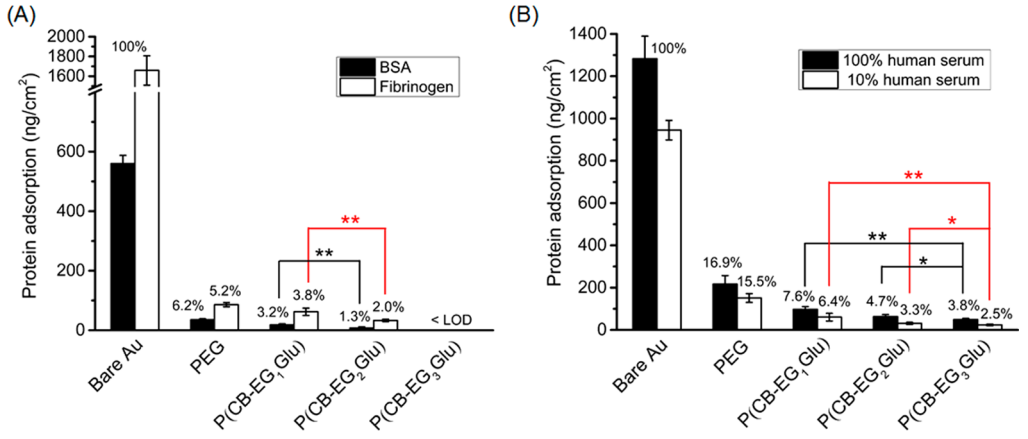

Figure 3. The amount of BSA, fibrinogen (A), and the dilute (10%) or complete (100%) human blood serum (B) adsorption on bare and different polymer-coated gold surfaces. The amount of protein adsorbed was measured by QCM and calculated based on the Voigt viscoelastic model. The data were further processed by normalizing to the amount of protein adsorption on the bare gold surface. LOD: the limit of detection. The p value ($^{*}p < 0.05$ and $^{**}p < 0.001$) was calculated by two-way ANOVA analysis.

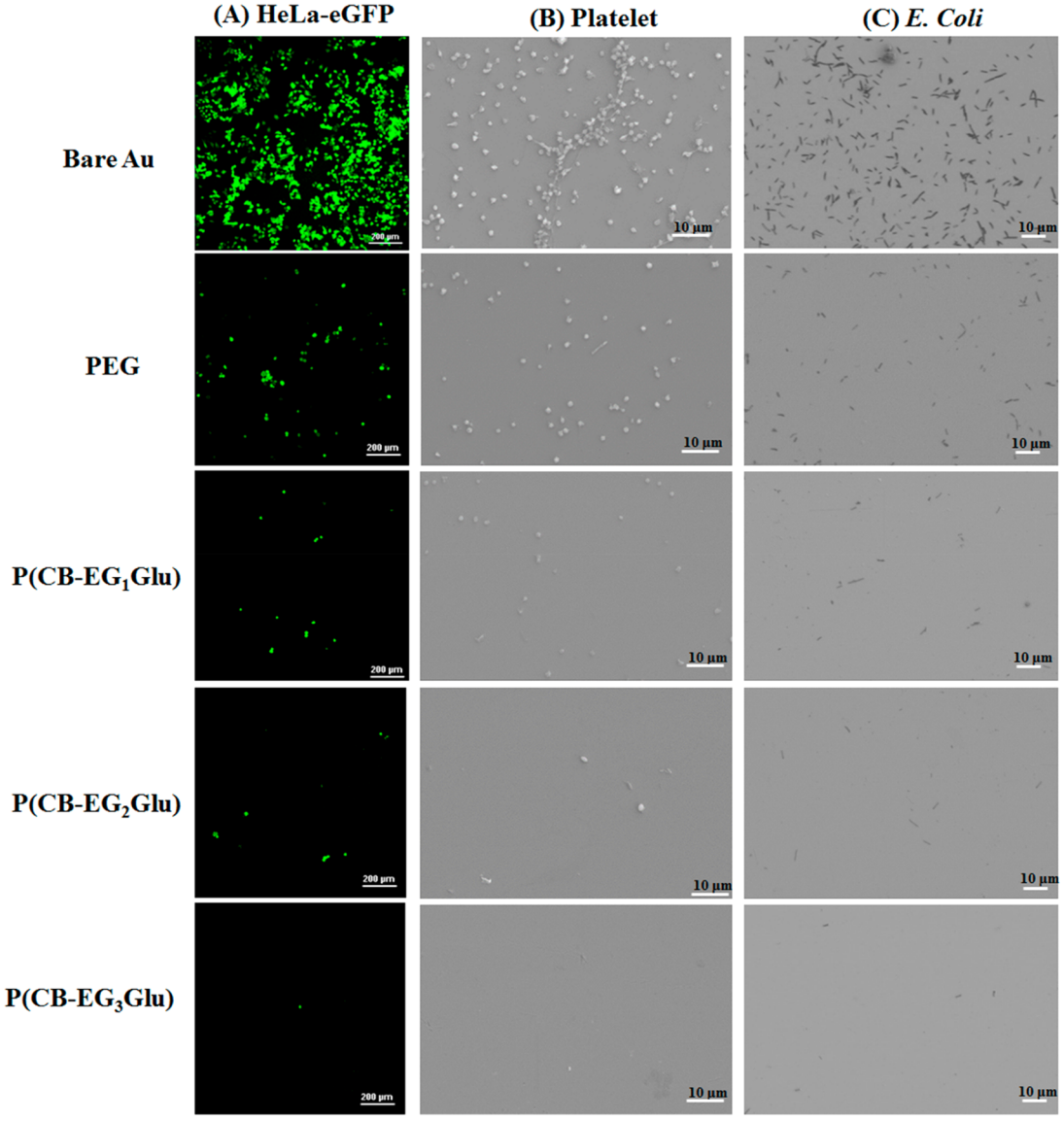

Figure 4. Cell adhesion prevention of the zwitterionic polypeptide- and PEG-coated surfaces. Representative Fluorescence images of eGFP-HeLa cells (A) and SEM images of platelets (B) and *E. coli* cells (C) adhered on bare and polymer-coated gold surfaces.

DOI: 10.1021/acsami.8b02854
ACS Appl. Mater. Interfaces 2018, 10, 17463−17470

than the thickness difference of the two in the dry state. Thus, it was hypothesized that the P(CB-EG_3Glu)-coated surface can absorb water more efficiently than the one coated with P(CB-EG_1Glu). To verify this, the wettability of the surfaces was evaluated by the static water contact angle (SCA) test (Figure 2C). The results indicated that the bare gold surface wettability increased dramatically after the adsorption of the zwitterionic polypeptides as shown by the plunge of the SCAs from ~85° to below 40°, which was presumably due to the ionic solvation. Moreover, the SCAs decreased consistently with the increased EG_x length, and P(CB-EG_3Glu) showed the smallest SCA (~30°) among all samples. We attributed this enhanced hydratability of P(CB-EG_3Glu) to the longer EG_x linker, which had literally 3 times more EG repeating units per residue and could thus compensate the effect of the decreased grafting density with respect to P(CB-EG_1Glu). To probe the secondary structure of surface-grafted polymers, we coated the polymers on quartz wafers (see Experimental Section) and measured their CD spectra. It was shown that all P(CB-EG_xGlu)-coated quartz wafers possess the characteristic α-helical conformation (Figure 2D), indicating the conformation of all polymers were well-preserved from solution to surface. Moreover, AFM examination of the surfaces demonstrated the uniformed structure of all coatings with a similar roughness below 0.8 (Figure S8).

Protein Resistance of the P(CB-EG_xGlu)-Coated Surfaces. The antifouling properties of the zwitterionic polypeptide-coated surfaces were first tested by the single protein (BSA or fibrinogen) adsorption assay using QCM-D (Figure 3A). The PEG-coated gold surface prepared under the same condition was selected to serve as the positive control. The results showed that the zwitterionic polypeptides coating significantly improved the protein resistance of the bare gold surface. Interestingly, the P(CB-EG_1Glu) coating demonstrated comparable capability in preventing BSA and fibrinogen adsorption in relative to the PEG control. Importantly, the amount of the adsorbed proteins decreased dramatically when the EG_x linker became longer. Particularly, P(CB-EG_3Glu) showed the best protein resistance among all tested samples. It was remarkably to found that the amount of both BSA and fibrinogen adsorbed on the P(CB-EG_3Glu)-coated surface were below the limit of detection of our QCM instrument (Figure 3A), which outperformed the PEG-coated surface with a wide margin.

Next, we tested our zwitterionic polypeptide coatings in dilute and complete human blood serum, a complex biological fluid containing various highly adhesive proteins.[46] Consistent with the single protein adsorption results described above, the zwitterionic polypeptide bearing the longest EG_3 linker showed the best nonfouling property (Figure 3B and Figure S9). Specifically, P(CB-EG_1Glu)-, P(CB-EG_2Glu)-, and P(CB-EG_3Glu)-coated surfaces exhibited an ~92–94%, ~95–97%, and ~96–98% reduction in the adsorption of human serum compared with that of bare gold, respectively. In contrast, the PEG coating reduced only ~83–85% protein adsorption under the same conditions.

Cell Adhesion. Apart from the protein resistance, the prevention of cell adhesion was another important indication of the nonfouling performance.[47] For this, we evaluated the cell adhesion behaviors of the zwitterionic polypeptide-coated surfaces using Hela-eGFP cells (Figure 4A), mouse platelets (Figure 4B), and *E. coli* bacterial cells (Figure 4C). The accumulated attachment of these cells, if untreated, would lead to serious problems including chronic inflammation, thrombosis, and biofilm formation.[3,5,48] Again, the P(CB-EG_3Glu)-coated surface was found to outperform all other samples, including the PEG-modified surface. Indeed, there were very few, if any, cells observed on the P(CB-EG_3Glu)-coated surface in our confocal and SEM studies (estimated >99% reduction, Figure S10), whereas all other polymer-coated surfaces tested in our study showed different degree of cell adhesion (~80–85% reduction for the PEG-coated surface). Overall, the cell adhesion results were in good agreement with those of the protein resistance studies described above.

CONCLUSIONS

In summary, we generate and compare a series of well-defined zwitterionic polypeptides bearing oligoethylene glycol linkers in the side chain. The polymers are anchored on gold surfaces via the grafting-to approach, and the surface properties are characterized by XPS, VASE, and SCA. By use of QCM, confocal microscopy, and SEM, our results convincingly demonstrate the excellent antifouling performance of all zwitterionic polypeptides. Importantly, the surface coated with P(CB-EG_3Glu), the one with the longest EG linker, exhibits the complete resistance to single protein and ~96–98% of plasma adsorption, which largely outperforms the performance of P(CB-EG_1Glu), P(CB-EG_2Glu), and the PEG positive control. The same P(CB-EG_3Glu) surface also gives the highest degree of prevention of cell/platelet/bacterial attachment and inhibition of biofilm formation among all samples tested. Apparently, this enhanced antifouling property of P(CB-EG_3Glu) is a result of its prolonged EG linker, which makes the surface more hydrophilic. This implied that the improved antifouling performance can be realized by the integration of hydrogen bonding induced hydration (EG_x) with ionic solvation. Nevertheless, because the longer EG_x linker can also lead to slightly decreased grafting density, one needs to be more careful when further growth of the EG_x linker is under consideration. Together, our study highlights the linker effect to the nonfouling performance of zwitterionic polypeptides, and the results strongly support P(CB-EG_3Glu) as a robust nonfouling material for numerous applications.

ASSOCIATED CONTENT

Supporting Information

The Supporting Information is available free of charge on the ACS Publications website at DOI: 10.1021/acsami.8b02854.

GPC, ^{1}H NMR, and helical stability characterization of zwitterionic polypeptides; XPS analysis, dry thickness and AFM 3D images of surface coating; QCD-D sensorgrams of serum adsorption and the quantified results of surface attached cells (PDF)

AUTHOR INFORMATION

Corresponding Author

*(H.L.) E-mail chemhualu@pku.edu.cn.

ORCID

Hua Lu: 0000-0003-2180-3091

Author Contributions

C.Z. and J.L. contributed equally.

Notes

The authors declare no competing financial interest.

DOI: 10.1021/acsami.8b02854
ACS Appl. Mater. Interfaces 2018, 10, 17463–17470

■ ACKNOWLEDGMENTS

This project was supported by National Natural Science Foundation of China (No. 21722401, 21474004, and 21434008). H.L. thanks the startup funding from Youth Thousand-Talents Program of China. We thank Dr. Wei Wei and Xiaodi Da for assistance with QCM-D and SEM test.

■ REFERENCES

(1) Liu, X.; Yuan, L.; Li, D.; Tang, Z.; Wang, Y.; Chen, G.; Chen, H.; Brash, J. L. Blood Compatible Materials: State of the Art. *J. Mater. Chem. B* **2014**, *2* (35), 5718−5738.
(2) Yang, W. J.; Neoh, K.-G.; Kang, E.-T.; Teo, S. L.-M.; Rittschof, D. Polymer Brush Coatings for Combating Marine Biofouling. *Prog. Polym. Sci.* **2014**, *39* (5), 1017−1042.
(3) Hall-Stoodley, L.; Costerton, J. W.; Stoodley, P. Bacterial Biofilms: from the Natural Environment to Infectious Diseases. *Nat. Rev. Microbiol.* **2004**, *2*, 95−108.
(4) Ma, C.; Xu, W.; Pan, J.; Xie, Q.; Zhang, G. Degradable Polymers for Marine Antibiofouling: Optimizing Structure To Improve Performance. *Ind. Eng. Chem. Res.* **2016**, *55* (44), 11495−11501.
(5) Banerjee, I.; Pangule, R. C.; Kane, R. S. Antifouling Coatings: Recent Developments in the Design of Surfaces That Prevent Fouling by Proteins, Bacteria, and Marine Organisms. *Adv. Mater.* **2011**, *23* (6), 690−718.
(6) Blaszykowski, C.; Sheikh, S.; Thompson, M. Surface Chemistry to Minimize Fouling from Blood-Based Fluids. *Chem. Soc. Rev.* **2012**, *41* (17), 5599−5612.
(7) Yu, Q.; Zhang, Y.; Wang, H.; Brash, J.; Chen, H. Anti-fouling Bioactive Surfaces. *Acta Biomater.* **2011**, *7* (4), 1550−1557.
(8) Krishnan, S.; Weinman, C. J.; Ober, C. K. Advances in Polymers for Anti-biofouling Surfaces. *J. Mater. Chem.* **2008**, *18* (29), 3405−3413.
(9) Wang, J.; Gibson, M. I.; Barbey, R.; Xiao, S. J.; Klok, H. A. Nonfouling Polypeptide Brushes *via* Surface-Initiated Polymerization of N^{ε}-oligo(ethylene glycol)succinate-$_{L}$-lysine *N*-carboxyanhydride. *Macromol. Rapid Commun.* **2009**, *30*, 845−850.
(10) Zhi, Z.; Su, Y.; Xi, Y.; Tian, L.; Xu, M.; Wang, Q.; Padidan, S.; Li, P.; Huang, W. Dual-Functional Polyethylene Glycol-*b*-Polyhexanide Surface Coating with in Vitro and in Vivo Antimicrobial and Antifouling Activities. *ACS Appl. Mater. Interfaces* **2017**, *9* (12), 10383−10397.
(11) Jiang, S.; Cao, Z. Ultralow-Fouling, Functionalizable, and Hydrolyzable Zwitterionic Materials and Their Derivatives for Biological Applications. *Adv. Mater.* **2010**, *22* (9), 920−932.
(12) Yang, W.; Xue, H.; Li, W.; Zhang, J.; Jiang, S. Pursuing "Zero" Protein Adsorption of Poly(carboxybetaine) from Undiluted Blood Serum and Plasma. *Langmuir* **2009**, *25* (19), 11911−11916.
(13) Kuang, J.; Messersmith, P. B. Universal Surface-Initiated Polymerization of Antifouling Zwitterionic Brushes Using a Mussel-Mimetic Peptide Initiator. *Langmuir* **2012**, *28* (18), 7258−7266.
(14) Liu, Q.; Singh, A.; Liu, L. Amino Acid-Based Zwitterionic Poly(serine methacrylate) as an Antifouling Material. *Biomacromolecules* **2013**, *14* (1), 226−231.
(15) Yang, W.; Zhang, L.; Wang, S.; White, A. D.; Jiang, S. Functionalizable and Ultra Stable Nanoparticles Coated with Zwitterionic Poly(carboxybetaine) in Undiluted Blood Serum. *Biomaterials* **2009**, *30* (29), 5617−5621.
(16) Hu, J.; Wang, G.; Zhao, W.; Gao, W. In Situ Growth of a C-terminal Interferon-alpha Conjugate of a Phospholipid Polymer That Outperforms PEGASYS in Cancer Therapy. *J. Controlled Release* **2016**, *237*, 71−77.
(17) Keefe, A. J.; Jiang, S. Poly(zwitterionic) Protein Conjugates Offer Increased Stability without Sacrificing Binding Affinity or Bioactivity. *Nat. Chem.* **2012**, *4*, 59−63.
(18) Kane, R. S.; Deschatelets, P.; Whitesides, G. M. Kosmotropes Form the Basis of Protein-Resistant Surfaces. *Langmuir* **2003**, *19* (6), 2388−2391.
(19) Shao, Q.; Jiang, S. Molecular Understanding and Design of Zwitterionic Materials. *Adv. Mater.* **2015**, *27* (1), 15−26.
(20) Zhao, C.; Zhao, J.; Li, X.; Wu, J.; Chen, S.; Chen, Q.; Wang, Q.; Gong, X.; Li, L.; Zheng, J. Probing Structure−Antifouling Activity Relationships of Polyacrylamides and Polyacrylates. *Biomaterials* **2013**, *34* (20), 4714−4724.
(21) Higaki, Y.; Inutsuka, Y.; Sakamaki, T.; Terayama, Y.; Takenaka, A.; Higaki, K.; Yamada, N. L.; Moriwaki, T.; Ikemoto, Y.; Takahara, A. Effect of Charged Group Spacer Length on Hydration State in Zwitterionic Poly(sulfobetaine) Brushes. *Langmuir* **2017**, *33* (34), 8404−8412.
(22) Fan, X.; Lin, L.; Messersmith, P. B. Cell Fouling Resistance of Polymer Brushes Grafted from Ti Substrates By Surface-Initiated Polymerization: Effect of Ethylene Glycol Side Chain Length. *Biomacromolecules* **2006**, *7* (8), 2443−2448.
(23) Song, Z.; Han, Z.; Lv, S.; Chen, C.; Chen, L.; Yin, L.; Cheng, J. Synthetic Polypeptides: from Polymer Design to Supramolecular Assembly and Biomedical Application. *Chem. Soc. Rev.* **2017**, *46* (21), 6570−6599.
(24) Lu, H.; Wang, J.; Song, Z.; Yin, L.; Zhang, Y.; Tang, H.; Tu, C.; Lin, Y.; Cheng, J. Recent Advances in Amino Acid *N*-carboxyanhydrides and Synthetic Polypeptides: Chemistry, Self-Assembly and Biological Applications. *Chem. Commun.* **2014**, *50* (2), 139−155.
(25) Shen, Y.; Fu, X.; Fu, W.; Li, Z. Biodegradable Stimuli-Responsive Polypeptide Materials Prepared by Ring Opening Polymerization. *Chem. Soc. Rev.* **2015**, *44* (3), 612−622.
(26) Zhang, C.; Lu, H. Efficient Synthesis and Application of Protein-Poly(α-amino acid) Conjugates. *Acta. Polym. Sin.* **2018**, No. 1, 21−31.
(27) Borase, T.; Heise, A. Hybrid Nanomaterials by Surface Grafting of Synthetic Polypeptides Using *N*-Carboxyanhydride (NCA) Polymerization. *Adv. Mater.* **2016**, *28* (27), 5725−5731.
(28) Shen, Y.; Li, Z.; Klok, H.-A. Polypeptide Brushes Grown *via* Surface-initiated Ring-Opening Polymerization of α-amino acid *N*-carboxyanhydrides. *Chin. J. Polym. Sci.* **2015**, *33* (7), 931−946.
(29) Hou, Y.; Yuan, J.; Zhou, Y.; Yu, J.; Lu, H. A Concise Approach to Site-Specific Topological Protein−Poly(amino acid) Conjugates Enabled by in Situ-Generated Functionalities. *J. Am. Chem. Soc.* **2016**, *138* (34), 10995−11000.
(30) Xia, H.; Fu, H.; Zhang, Y.; Shih, K.-C.; Ren, Y.; Anuganti, M.; Nieh, M.-P.; Cheng, J.; Lin, Y. Supramolecular Assembly of Comb-Like Macromolecules Induced by Chemical Reactions that Modulate the Macromolecular Interactions In Situ. *J. Am. Chem. Soc.* **2017**, *139* (32), 11106−11116.
(31) Wibowo, S. H.; Sulistio, A.; Wong, E. H. H.; Blencowe, A.; Qiao, G. G. Polypeptide Films *via* *N*-carboxyanhydride Ring-Opening Polymerization (NCA-ROP): Past, Present and Future. *Chem. Commun.* **2014**, *50* (39), 4971−4988.
(32) Deming, T. J. Synthesis of Side-Chain Modified Polypeptides. *Chem. Rev.* **2016**, *116* (3), 786−808.
(33) Xuan, S.; Gupta, S.; Li, X.; Bleuel, M.; Schneider, G. J.; Zhang, D. Synthesis and Characterization of Well-Defined PEGylated Polypeptoids as Protein-Resistant Polymers. *Biomacromolecules* **2017**, *18* (3), 951−964.
(34) Zhang, C.; Yuan, J.; Lu, J.; Hou, Y.; Xiong, W.; Lu, H. From neutral to zwitterionic poly (α-amino acid) nonfouling surfaces: Effects of helical conformation and anchoring orientation. *Biomaterials* **2018**, DOI: 10.1016/j.biomaterials.2018.01.052.
(35) Hashim, P. K.; Okuro, K.; Sasaki, S.; Hoashi, Y.; Aida, T. Reductively Cleavable Nanocaplets for siRNA Delivery by Template-Assisted Oxidative Polymerization. *J. Am. Chem. Soc.* **2015**, *137* (50), 15608−15611.
(36) Yuan, J.; Zhang, Y.; Sun, Y.; Cai, Z.; Yang, L.; Lu, H. Salt- and pH-Triggered Helix-Coil Transition of Ionic Polypeptides under Physiology Conditions. *Biomacromolecules* **2018**, DOI: 10.1021/acs.biomac.8b00204.
(37) Shen, Y.; Desseaux, S.; Aden, B.; Lokitz, B. S.; Kilbey, S. M.; Li, Z.; Klok, H.-A. Shape-Persistent, Thermoresponsive Polypeptide Brushes Prepared by Vapor Deposition Surface-Initiated Ring-

DOI: 10.1021/acsami.8b02854
ACS Appl. Mater. Interfaces 2018, 10, 17463−17470

Opening Polymerization of α-Amino Acid *N*-Carboxyanhydrides. *Macromolecules* **2015**, *48* (8), 2399−2406.
(38) Hilfiker, J. N.; Synowicki, R. A. Spectroscopic Ellipsometry for Polymer Thin Films. *Solid State Technol.* **1998**, *41*, 101−110.
(39) Biggs, C. I.; Walker, M.; Gibson, M. I. "Grafting to" of RAFTed Responsive Polymers to Glass Substrates by Thiol−Ene and Critical Comparison to Thiol−Gold Coupling. *Biomacromolecules* **2016**, *17*, 2626−2633.
(40) Reviakine, I.; Johannsmann, D.; Richter, R. P. Hearing What You Cannot See and Visualizing What You Hear: Interpreting Quartz Crystal Microbalance Data from Solvated Interfaces. *Anal. Chem.* **2011**, *83*, 8838−8848.
(41) Wei, Q.; Becherer, T.; Noeske, P.-L. M.; Grunwald, I.; Haag, R. A Universal Approach to Crosslinked Hierarchical Polymer Multilayers as Stable and Highly Effective Antifouling Coatings. *Adv. Mater.* **2014**, *26*, 2688−2693.
(42) Gillich, T.; Benetti, E. M.; Rakhmatullina, E.; Konradi, R.; Li, W.; Zhang, A.; Schlüter, A. D.; Textor, M. Self-Assembly of Focal Point Oligo-Catechol Ethylene Glycol Dendrons on Titanium Oxide Surfaces: Adsorption Kinetics, Surface Characterization, and Nonfouling Properties. *J. Am. Chem. Soc.* **2011**, *133* (28), 10940−10950.
(43) Lu, H.; Wang, J.; Bai, Y.; Lang, J. W.; Liu, S.; Lin, Y.; Cheng, J. Ionic Polypeptides with Unusual Helical Stability. *Nat. Commun.* **2011**, *2*, 206.
(44) Chastain, J.; King, R. C.; Moulder, J. *Handbook of X-ray Photoelectron Spectroscopy: A Reference Book of Standard Spectra for Identification and Interpretation of XPS Data*; Physical Electronics Division, Perkin-Elmer Corporation: Eden Prairie, MN, 1992.
(45) Yang, W. J.; Neoh, K.-G.; Kang, E.-T.; Lay-Ming Teo, S.; Rittschof, D. Stainless Steel Surfaces with Thiol-Terminated Hyperbranched Polymers for Functionalization *via* Thiol-Based Chemistry. *Polym. Chem.* **2013**, *4* (10), 3105−3115.
(46) Gunkel, G.; Huck, W. T. S. Cooperative Adsorption of Lipoprotein Phospholipids, Triglycerides, and Cholesteryl Esters Are a Key Factor in Nonspecific Adsorption from Blood Plasma to Antifouling Polymer Surfaces. *J. Am. Chem. Soc.* **2013**, *135* (18), 7047−7052.
(47) Koegler, P.; Clayton, A.; Thissen, H.; Santos, G. N. C.; Kingshott, P. The Influence of Nanostructured Materials on Biointerfacial Interactions. *Adv. Drug Delivery Rev.* **2012**, *64* (15), 1820−1839.
(48) Ding, X.; Yang, C.; Lim, T. P.; Hsu, L. Y.; Engler, A. C.; Hedrick, J. L.; Yang, Y.-Y. Antibacterial and Antifouling Catheter Coatings Using Surface Grafted PEG-*b*-Cationic Polycarbonate Diblock Copolymers. *Biomaterials* **2012**, *33* (28), 6593−6603.

DOI: 10.1021/acsami.8b02854
ACS Appl. Mater. Interfaces 2018, 10, 17463−17470